Adsorption of CO_2/CH_4 Mixtures in a Molecular Model of Activated Carbon through Monte Carlo Simulations†

Alberto G. Albesa[1,*], Matías Rafti[1], José L. Vicente[1], Hernán Sánchez[1], Pablo Húmpola[2]

(1) Instituto de Investigaciones Fisicoquímicas Teóricas y Aplicadas (INIFTA) UNLP-CIC-CONICET, Casilla de Correo 16, Sucursal 4, 1900 La Plata, Argentina. (2) Cátedra de Química Inorgánica, Facultad de Bioquímica y Ciencias Biológicas, Universidad del Litoral, CC242 3000, Santa Fe, Argentina.

(Received 25 July 2012; revised form accepted 8 October 2012)

ABSTRACT: In this article, a nanoporous carbon model based on units of polyaromatic molecules with different number of rings is described. The adsorption isotherms of pure CO_2, CH_4 and equimolar mixtures, and isosteric heat calculations on these models substrates were obtained by Monte Carlo simulations. The results were analyzed in the framework of dual process Langmuir model (DPL) and on the basis of ideal adsorption solution theory. We found that both methods predict the adsorption isotherms of mixtures based on pure components data with reasonable accuracy. It has been demonstrated that the isosteric heat and selectivity of a mixture are intimately related. The DPL model does not predict the correct numerical value of selectivities; however, it predicts the correct behaviour. This is very useful as a fast method to indicate the adsorption behaviour of mixtures.

1. INTRODUCTION

In the last four decades there had been an increasing interest to develop new separation and purification techniques including adsorption using various adsorbents. One of the principal uses of adsorption is the separation of impurities in contaminated gases (Sircar 2006). This kind of removal is computerized, wherein the subroutine computing the adsorption in equilibrium state plays an important role. The accuracy of predicted values and the speed of calculations will be reflected in the purity of the separated gases. Because adsorption is affected by enthalpic effects, it is important to consider these effects, as they have an important impact on the efficiency of such processes (Nieszporek 2006).

Predicting the adsorption behaviour of mixtures from pure component data is very important, from both the theoretical and practical viewpoints. Constructing new adsorption models had attracted great deal of attention (Ayappa 1998), and these models were developed for either homogeneous adsorbents (Lee and O'Connell 1974) or completely heterogeneous adsorbents (Azizian and Bashiri 2009). However, these studies are about monolayer adsorption and about the few existing models of multi-layer mixture adsorption (Kruk *et al*. 1995; Grabowski *et al*. 2000; Woywod and Schoen 2003). It is evident that adsorption is a versatile tool for the separation and purification of industrial mixtures. However, at present, experimental data on mixed systems are

†First presented at the joint 1st Ibero-American Symposium on Adsorption (IBA1) & 9th Brazilian Meeting on Adsorption (EBA9), Recife, Brazil, 6–10 May 2012

*Author to whom all correspondence should be addressed. E-mail: albesa@inifta.unlp.edu.ar

very limited. To cope up with this limitation, empirical or theoretical models are used to estimate desired multi-component equilibrium data in practical applications. From the above discussed facts, there is a need to address the following issues:

1. To test existing models of multi-component adsorption.
2. To develop new models or improve the existing models.
3. To provide better understanding of the phenomena during the adsorption of multi-component systems.
4. To study the effect of dimensionality, temperature, pore size and the potential separation.

Describing the adsorption of carbon dioxide, methane and their binary mixtures on activated carbons allows for focusing on some interesting problems of current research. First, from the technological perspective, both carbon dioxide and methane have been related to the greenhouse effect. The technology for controlling CO_2 emissions involves preferential adsorption from gaseous mixtures. In addition, mixtures of hydrocarbons with CO_2 occur in natural gas, and are also an important constituent in enhanced oil recovery technology. Adsorption techniques (e.g. membrane and pressure swing methods) together with porous adsorbents, especially carbons, seem to be promising candidates for these separations. However, it is still very difficult to evaluate the adsorption capacity of activated carbons in separation techniques because of the non-trivial problem of adsorption behaviour prediction of mixtures. What is lacking is a suitable model for the internal structure of carbon. If the internal structure of a specific activated carbon could be modelled, then prediction of the adsorption by molecular simulation could be achieved.

Porous carbons are, in general, disordered materials and yet cannot be fully characterized from experiments. Realistic molecular models of these materials are needed to understand experimental data used to characterize the pore structure of carbons, as well as to predict a wide range of properties (adsorption, heats of adsorption, diffusion rates, etc.) of confined phases within carbons. The most commonly used model for porous carbons is the slit-pore model (Pikunic *et al*. 2003) in which the carbon is represented with stacks of infinite graphene layers, separated by slit-shaped pores. The heterogeneity of the material is thus represented by a range of pore widths. However, the slit-pore model fails to account for pore connectivity or tortuosity, or for the curved and defective graphene segments that are shown by X-ray and high-resolution transmission electron microscopy studies. Consequently, it fails to account correctly for adsorption (Coasne *et al*. 2003) and it is particularly inadequate for predicting heats of adsorption or diffusion in these materials.

The inability of single-pore models to capture these and other important phenomena has motivated the development of molecular models of carbons that include the complexity of real carbons: Seaton *et al*. (1997) developed a variation of the slit-pore model to try to account for surface irregularities; Segarra and Glandt (1994) modelled the microstructure as a collection of cylindrical disk of specific thickness; Dahn *et al*. proposed a model based on the observation that the increase in graphene layering during pyrolisis of specific carbon formulation was accompanied by increased pore sizes (Dahn *et al*.. 1997); Acharya *et al*. (1999) presented a model for nanoporous carbon based on chemical constraints, while Thomson and Gubbins (2000) used the reverse Monte Carlo method for modelling the microstructure of activated carbons. Another perspective is the quench molecular dynamics method, which aims to build structural models from the ground up, predicting the nanostructure and porous features of disordered nanoporous carbons using techniques that are rooted in statistical mechanics (Palmer and Gubbins 2012). More recently Kumar *et al*. have considered an *in silico*-generated random structure that can be taken as a model of real carbons to study the hydrogen physisorption and chemisorption in nanoporous

carbon structures (Kumar *et al*. 2011) and the adsorption of methane/hydrogen mixtures on carbon micropores (Kumar *et al*. 2012).

A widely used interpretation of experimental data is the hierarchical structure. The so-called basic structural unit (BSU) is the fundamental building block of activated carbons. The BSU consists of a few roughly aligned small polyaromatic molecules. The size of the BSU is in the scale of the nanometre. There is an absence of graphite-like order between the layers within a BSU, and the inter-layer spacing is greater than that of graphite. The BSUs are assembled to form regions of local molecular orientation which are in turn assembled in the space to yield the complex structures of activated carbon (Bandosz *et al*. 2003).

Because the model of the surface plays an important role for the gas adsorption even for very simple adsorbates such as graphite (Albesa *et al*. 2008), in this work we describe a nanoporous carbon model that consists of units of polyaromatic molecules with different number of rings in order to get different BSUs. One of the main techniques used in adsorption studies is Monte Carlo simulations (MCS) with the Grand Canonical Ensemble (Bottani 1999) because MCS offer the possibility of studying the phenomenon at the molecular level (microscopic). By specifying the chemical potential, temperature and volume of the pore, the grand canonical MCS can be used to effectively calculate the adsorption capacity of the pores. The number of particles is then obtained from the simulation for a given chemical potential (Do and Do 2003). In this work, the adsorption of equimolar binary mixtures of methane and carbon dioxide is simulated in a molecular model of activated carbon with clusters of 24, 54, 96 and 150 carbon atoms. We show how the cluster size affects adsorption selectivity.

2. METHODOLOGY

2.1. Methodology to Simulate the Activated Carbon

In this work, two-dimensional clusters of polyaromatic molecules consisting of 24, 54, 96 and 150 carbon atoms were used to simulate the surface. The apparent density simulated was 1.0 g/cm^3. The method to stimulate activated carbon is as follows:

1. The simulation box was filled with one kind of cluster parallel to the *xy* plane until the desired density was achieved.
2. The clusters were randomly moved along the *x*, *y* and *z* axis and could be rotated at an angle of 10°.
3. The energy of the model was calculated and saved, using the Hyperchem and the MM+ level. These steps were repeated 1500 times for each kind of cluster and density. The result was 6000 active carbon models. The models displaying the lowest energy were subjected to a geometry optimization, and finally used as adsorbents in this work and labelled as C-24-1, C-54-1, C-96-1 and C-150-1 (where the first number is the carbon atom in the cluster and the second number is the density of the simulated activated carbon) (Figures 1 and 2).

2.2. Structural Information of the Carbons

The main characteristics of these molecular models were described elsewhere (Albesa 2010), and only a brief summary is provided here.

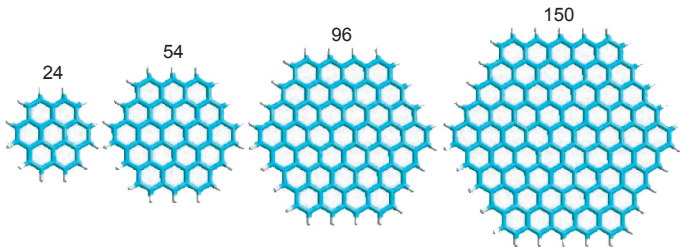

Figure 1. Polyaromatic clusters used to simulate the activated carbons structures.

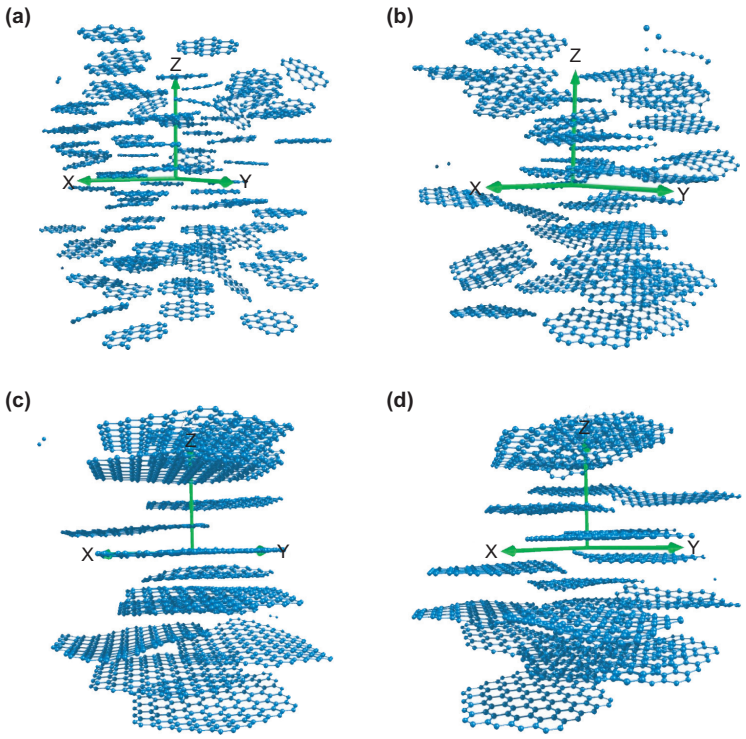

Figure 2. Structures for the simulated carbons. (a) C-24-1; (b) C-54-1; (c) C-96-1; (d) C-150-1.

2.3. Pair Distribution Function

The most commonly used structural properties in reverse Monte Carlo methods are the structure factor, S(q), and the pair distribution function (PDF), g(r) (Palmer *et al*. 2009), which are usually obtained from X-ray diffraction and neutron scattering experiments (Smith *et al*. 2004). One of the key advantages of building structural models for activated carbons is that their microstructure features can be examined by exact geometric methods and the calculation of the PDF is straightforward.

2.3. Surface Area

The specific surfaces of the substrates are determined using the Brunauer–Emmett–Teller (BET) model in the linear region of the isotherms (P/P_0 between 0.05 and 0.35). In order to the calculate BET area, we simulated nitrogen isotherms at 77 K.

2.4. MCSs

The parameters used in all the MCSs presented in this work are as follows:

1. The length of the side of the simulation box, 10 $\sigma_{methane}$
2. The cut-off radius, 4 $\sigma_{methane}$
3. 2.5×10^6 Monte Carlo steps were used for thermalization (including creation, destruction or displacement attempts for each molecule); these were followed by 5×10^4 steps for determining the statistical averages.

In this article, methane and carbon dioxide are used and their pair-wise potential of interaction is described by the one-centre Lennard–Jones (LJ) model. The LJ parameters listed in Table 1 and cut-off radius that is four times the collision diameter ($4\sigma_{ff}$) is used. The potential energy of interaction between two fluid particles is calculated using the following LJ (12,6) equation:

$$_{ff}(r) = 4\varepsilon_{ff}\left[\left(\frac{\sigma_{ff}}{r}\right)^{12} - \left(\frac{\sigma_{ff}}{r}\right)^{6}\right] \tag{1}$$

where r is the separation distance between the two particles.

The interaction energy between a fluid particle and a carbon atom is calculated by the same equation, equation (1), with σ_{ff} and ε_{ff} being replaced by σ_{sf} and ε_{sf}, respectively. These cross-molecular parameters are calculated from the usual Lorentz–Berthelot rule. The accuracy and advantages of the adsorption potential given in equation (2) are well known.

$$\varepsilon_{sf} = \left(\varepsilon_{ss}\varepsilon_{ff}\right)^{12}, \quad \sigma_{sf} = \frac{1}{2}\left(\sigma_{ss} + \sigma_{ff}\right) \tag{2}$$

Assuming that the pair-wise addition holds, the total energy is calculated by summing the pair-wise interactions between fluid particles, and between individual carbon atoms and fluid particles as follows:

$$U = \sum_{i,j>i} {}_{ij}\left(\left|r_i - r_j\right|\right) + \sum_{i,k} {}_{ik}\left(\left|r_i - r_k\right|\right) \tag{3}$$

TABLE 1. Lennard–Jones Interaction Parameters

	$\varepsilon_{XX/kB}$	$\sigma_{XX/Å}$
Methane(X = f)	148.1 (Do and Do 2005)	3.81
Carbon dioxide (X = f)	246 (Ravikovitch *et al*. 2001)	3.648
Nitrogen (X = f)	71.4 (Takaba *et al*. 2002)	3.80
Graphite (X = s)	28 K	3.40

where r_i and r_j are the positions of fluid particles i and j, respectively, r_k is that of a carbon atom, φ_{ij} is the pair interaction potential energy between fluid particles and φ_{ik} is the pair interaction potential energy between particle i and carbon atom k.

2.5. Isosteric Heat of Adsorption

The isosteric heat of adsorption for the ith component of an ideal gas mixture ($q_{st,i}$) can be calculated using the following expression (Albesa *et al*. 2012):

$$\frac{q_{st,j}}{RT^2} = \left[\frac{d \ln p_i}{dT}\right]_{n_i} \tag{4}$$

where $p_i = Py_i$ represents the partial pressure of the ith component (P and y_i are total gas pressure and molar fraction in gas phase) in equilibrium with n_i moles in the adsorbed phase, T is the temperature and R is the gas constant. However, as previously noted, equation (4) is not a practical method for calculating the isosteric heat because the data required for using equation (4) are rarely found in the literature.

In MCSs the isosteric heat can be calculated from according to the procedure detailed by Karavias and Myers (1991):

$$q_{st,i} = \left(H^b - H^{*,b}\right) + RT - \left(\frac{\partial U^{a,c}}{\partial N^a}\right)_{T,V^a} \tag{5}$$

where the superscripts a, b and *, respectively, denote the value of the thermodynamic functions for the adsorbed, gas and ideal phases. $U^{a,c}$ is the configurational part of the interaction energy, which includes both adsorbate–adsorbate and adsorbate–adsorbent interactions. Assuming that the gas behaves as an ideal gas, equation (5) becomes:

$$q_{st,i} = RT - \left(\frac{\partial U^{a,c}}{\partial N^a}\right)_{T,V^a} \tag{6}$$

Here $\partial U^{a,c}/\partial N^a$ can be obtained either by numerical differentiation or from fluctuation theory:

$$\left(\frac{\partial U^{a,c}}{\partial N^a}\right) = \frac{f(U,N)}{f(N,N)} \quad \text{where} \quad f(X,Y) = \langle XY\rangle - \langle X\rangle\langle Y\rangle \tag{7}$$

Here the brackets, <X>, indicate the mean value of the quantity X.

The heat of adsorption of the ith component of a binary mixture can be obtained from the simulations by solving the following expressions:

$$q_{st,i} = RT - \left(\frac{\partial U^{a,c}}{\partial N_i^a}\right)_{T,V^a,N_{j\neq i}^a} \tag{8}$$

$$\left(\frac{\partial U^{a,c}}{\partial N^{a}}\right)=\sum_{k}\left(\frac{\partial U^{a,c}}{\partial \beta\mu_{k}}\right)_{T,V^{a},N^{a}_{j\neq i}}\left(\frac{\partial \beta\mu_{k}}{\partial N^{a}_{i}}\right)_{T,V^{a},N^{a}_{j\neq i}} \tag{9}$$

where

$$\left(\frac{\partial U^{a,c}}{\partial \beta\mu_{k}}\right)_{T,V^{a},N^{a}_{j\neq i}}=f\left(U,N^{a}_{k}\right) \tag{10}$$

$$\begin{pmatrix}\frac{\partial \beta\mu_{1}}{\partial U^{a}_{1}} & \frac{\partial \beta\mu_{1}}{\partial U^{a}_{2}}\\ \frac{\partial \beta\mu_{2}}{\partial U^{a}_{1}} & \frac{\partial \beta\mu_{2}}{\partial U^{a}_{2}}\end{pmatrix}=\begin{pmatrix}f\left(N^{a}_{1},N^{a}_{1}\right) & f\left(N^{a}_{1},N^{a}_{2}\right)\\ f\left(N^{a}_{2},N^{a}_{1}\right) & f\left(N^{a}_{2},N^{a}_{2}\right)\end{pmatrix}^{-1} \tag{11}$$

The isosteric heat of adsorption of the components of a gas mixture is a helpful quantity for understanding selectivity of a given adsorbent. The selectivity $S_{i,j}$ of the ith species relative to the jth species can be defined as follows:

$$S_{ij} = (\theta_i/\theta_j)/(p_i/p_j) \tag{12}$$

Here θ_i and θ_j are loading for species i and j, and p_i and p_j are the corresponding partial pressures.

2.6. Dual Process Langmuir Formulation

The single-gas dual process Langmuir (DPL) model describes the adsorption of component i on a heterogeneous adsorbent surface that is composed of two homogeneous but energetically different types of patches (or sites). Assuming that the adsorbate–adsorbent free energy on each patch is constant, the amount (n_i) adsorbed for component i is given by the following equation:

$$n_i=\left(\frac{n^{s}_{1,i}b_{1,i}P}{1+b_{1,i}P}\right)+\left(\frac{n^{s}_{2,i}b_{2,i}P}{1+b_{2,i}P}\right) \tag{13}$$

where $n_{1,i}^{s}$ and $b_{1,i}$ are the saturation capacity and affinity parameter on site 1, respectively, while $n_{2,i}^{s}$ and $b_{2,i}$ are the saturation capacity and affinity parameter on site 2, respectively, and P is the absolute pressure. All the assumptions of the Langmuir model apply to each patch, and the two patches do not interact with each other.

The extension of equation (13) to a binary system is straightforward. When both components can access both site 1 as a high-free-energy site (j = 1) and site 2 as a low-free-energy site (j = 2), then their adsorbate–adsorbent free energies correlate in a perfect positive (PP) fashion. However, when component A can only access site 1 as a high-free-energy site (j = 1), and component B can only access site 1 as a low-free-energy site (j = 2), and vice versa for site 2, then adsorbate–adsorbent free energies correlate in a perfect negative (PN) fashion. A PP correlation

arises from similarly sized species, perhaps with similar adsorbent affinities, and a PN correlation arises from differently sized species, with presumably dissimilar adsorbent affinities.

When components A and B obey the PP correlation for energetic site matching, the corresponding amount adsorbed for each component is given by

$$n_{A,m} = \left(\frac{n^s_{1,A} b_{1,A} P_{yA}}{1 + b_{1,A} P_{yA} + b_{1,B} P_{yB}} \right) + \left(\frac{n^s_{2,A} b_{2,A} P_{yA}}{1 + b_{2,A} P_{yA} + b_{2,B} P_{yB}} \right) \tag{14}$$

$$n_{B,m} = \left(\frac{n^s_{1,B} b_{1,B} P_{yB}}{1 + b_{1,A} P_{yA} + b_{1,B} P_{yB}} \right) + \left(\frac{n^s_{2,B} b_{2,B} P_{yB}}{1 + b_{2,A} P_{yA} + b_{2,B} P_{yB}} \right) \tag{15}$$

In contrast, when components A and B obey the PN correlation for energetic site matching, the corresponding amount adsorbed for each component is given by the following equations:

$$n_{A,m} = \left(\frac{n^s_{1,A} b_{1,A} P_{yA}}{1 + b_{1,B} P_{yA} + b_{2,B} P_{yB}} \right) + \left(\frac{n^s_{2,A} b_{2,A} P_{yA}}{1 + b_{2,B} P_{yA} + b_{1,B} P_{yB}} \right) \tag{16}$$

$$n_{B,m} = \left(\frac{n^s_{1,B} b_{1,B} P_{yB}}{1 + b_{2,A} P_{yA} + b_{1,B} P_{yB}} \right) + \left(\frac{n^s_{2,B} b_{2,B} P_{yB}}{1 + b_{1,A} P_{yA} + b_{2,B} P_{yB}} \right) \tag{17}$$

where y_A and y_B are the gas-phase mole fractions of components A and B and n_A and n_B are the adsorbed amounts of components A and B from a binary gas mixture. The total amount adsorbed is simply the sum of $n_{A,m}$ and $n_{B,m}$

2.8. Ideal Adsorption Solution Theory

The ideal adsorption solution theory (IAST) was developed by Myers and Prausnitz (Myers and Prausnitz 1965) and is widely used to predict the adsorption of mixtures from the data of the pure components. IAST is an analogue of Raoult's Law for vapour–liquid equilibrium and assumes that the adsorbed mixture is an ideal solution. Therefore, for a component i in an ideal solution with mole fraction x_i:

$$p_i = p_i^0(\pi)_i \tag{18}$$

where p_i is the partial pressure of component i and $p_i^0(\pi)$ is the pressure of the pure component i at the same spreading pressure π of the mixture. The spreading pressure per unit area is related to p_i^0 by the Gibbs adsorption isotherm

$$\pi = RT \int_0^{p_i^0} n_i(p) d\ln p \tag{19}$$

where n_i (p) is the adsorption isotherm of pure component i given by any isotherm that fits well with the experimental data. The amount of gas adsorbed can be calculated by the expression:

$$n_{i,m} = \frac{x_i}{\sum x_k / n_k^0(p_k^0)} \tag{20}$$

At a given pressure and composition, equations (18–20) can be solved together with the identity:

$$\sum_i \frac{p_{i0}}{p_i^0(\pi)} = 1 \tag{21}$$

to obtain the adsorbed amount of the individual components in a mixture. In general, the presented set of equations cannot be solved analytically and therefore must be solved numerically. However, the spreading pressure can be calculated analytically for the Toth isotherm, which is an empirical isotherm that satisfies the limits of low and high pressures. Is useful to describe systems in the area of submonolayer and has the following form:

$$n_i = \frac{n_{max} bP}{\left[1+(bP)^t\right]^{1/t}} \tag{22}$$

The parameters n_{max}, t, P, b are characteristic of each adsorbate–adsorbent system. As the parameter t moves away from the unit, the system is more heterogeneous.

3. RESULTS AND DISCUSSION

3.1. PDF and Surface Area

Figure 3 shows the PDF for the different models considered. It can be noticed that in all models the first peaks positions agree. The PDF obtained coincides with others obtained experimentally by X-ray (Buriana *et al*. 1998; Pikunic *et al*. 2003; Kumar *et al*. 2005; Nguyen *et al*. 2008). These peaks can be attributed to the distances between the carbon atoms within each of the clusters considered. At greater distances, the information that can be obtained depends on the size of the cluster considered. For the smaller clusters, it is not possible to obtain information beyond 7 Å, which coincides with the cluster size, indicating that these models are highly disordered. From PDFs it is not possible to obtain information about inter-cluster structure because, as stated earlier, all models have different structures and surface areas, and yet have similar PDFs. The most valuable information that can be obtained from the PDF is the size of the clusters that comprise the activated carbon. The specific surfaces of the substrates are determined using the BET model, in the linear region of the isotherms (p/p_0 between 0.05 and 0.35). The results are presented in Table 2 and they are in good agreement with the experimental models.

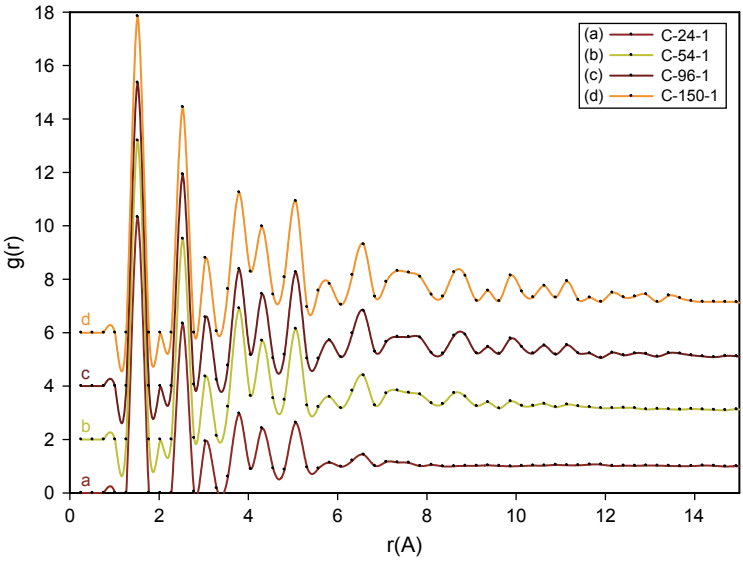

Figure 3. Calculated pair distribution functions.

TABLE 2. Specific Areas for the Simulated Activated Carbons

Cluster size	24	54	96	150
Specific surface area (m^2/g)	854	981	810	773

3.2. Pure Components Isotherms

The adsorption isotherms are shown in Figure 4. In methane isotherms it is observed that, in general, as the cluster size increases there is also an increase in the adsorption capacity throughout the pressure range. However, there is an exception with the C-96-1 and the C-150-1 isotherms, wherein C-96-1 shows greater adsorption capacity than C-150-1.

In contrast, the carbon dioxide isotherms show a different behaviour. At low pressures, the adsorption capacity shows the same trend as that of the methane isotherms. However, at higher pressures, the activated carbon that has the greater adsorption capacity is C-54-1.

This behaviour of the isotherms is reflected in the b parameters of the dual Langmuir and Toth isotherms, which are shown in Tables 3 and 4, respectively.

The data obtained from dual Langmuir model show that in the case of methane there is an agreement between the energies of sites in both low energy and high energy. However, this agreement is not retained in the case of carbon dioxide isotherms. At low pressures, i.e. in the areas with higher b, the behaviour is the same as that of methane and at high pressures (sites with low b), the parameter b of the activated carbon C-54-1 is larger than that of the carbons C-96-1 and C-150-1.

3.3. Isosteric Heat

Figure 5 shows total isosteric heats of adsorption and the fluid–fluid contribution from simulations, which were calculated using equation (6). The difference in the isosteric heat between the activated carbon models is basically due to fluid–solid contribution, because the fluid–fluid contribution is the same in all models. Based on the isosteric heat, we can define two types of

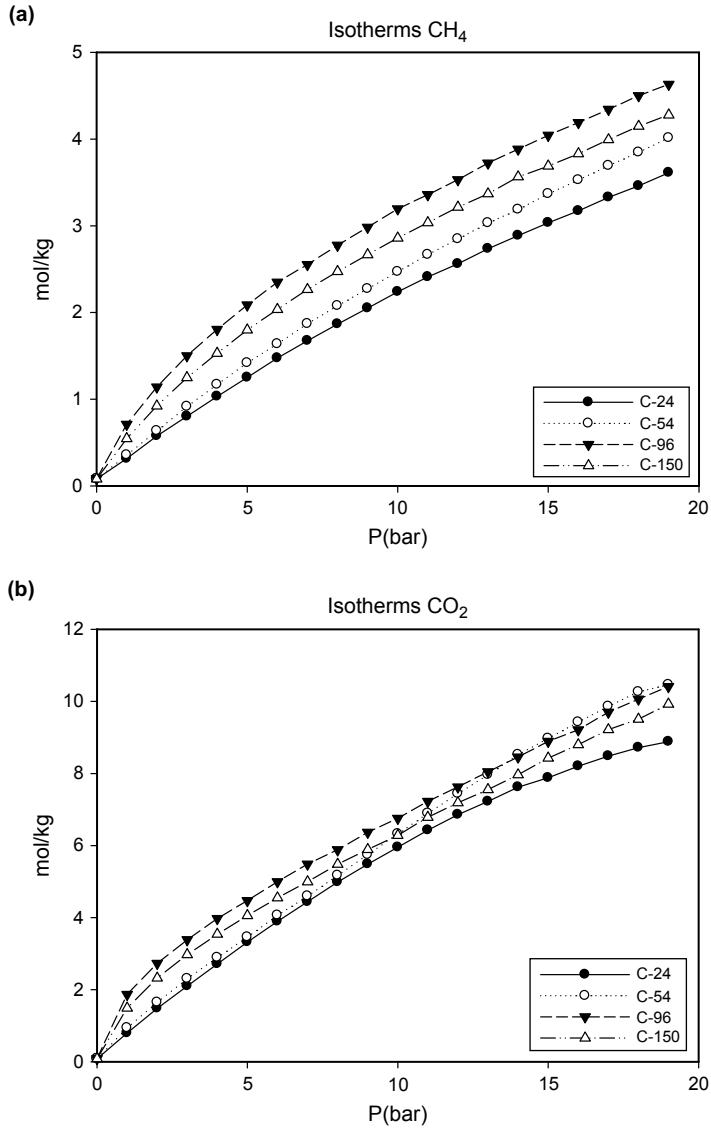

Figure 4. Simulated isotherms for simulated carbons at 298 K (a) CH_4; (b) CO_2.

sites. At low pressures, adsorption sites are formed by small slit-pores formed between different clusters, and the presence of this kind of sites is higher in the models C-96-1 and C-150-1. At higher pressures, however, the adsorption sites are pores formed by the edges of the clusters. The models C-24-1 and C-54-1 have more edges, and therefore, there is an increase in the isosteric heat in these models at high pressure. The energetic difference in the first kind of sites is observed for both gases. However, the energetic difference in the second kind of sites cannot be observed in the methane isosteric heat. The values of the isosteric heat obtained with these models are lower than the values reported in the literature. This can be explained taking into account that this model does not present high energy sites of adsorption such as oxygenated groups.

TABLE 3. Dual Langmuir Parameters

CH_4				
	n^s_1	b_1	n^s_2	b_2
C-24	3.2963	0.05123	12.3927	0.0099209
C-54	1.496	0.10361	18.4368	0.010247
C-96	1.2833	0.54388	12.5357	0.020058
C-150	1.2248	0.33744	13.4151	0.016598
CO_2				
	n^s_1	b_1	n^s_2	b_2
C-24	10.6817	0.035929	11.7006	0.035929
C-54	19.105	0.025528	27.7123	0.0099445
C-96	2.4575	1.3098	60.771	0.0080218
C-150	2.0622	0.99357	59.4534	0.0081241

TABLE 4. Toth Parameters

CH_4			
	n_{max}	b	t
C-24	27.3017	0.012104	0.6137
C-54	41.4602	0.0094897	0.53665
C-96	88.5467	0.024247	0.27216
C-150	58.4773	0.017232	0.34547
CO_2			
	n_{max}	b	t
C-24	13.0501	0.053735	1.7927
C-54	107.0139	0.0079068	0.63791
C-96	480.7077	0.013264	0.22269
C-150	413.8745	0.0078334	0.25866

3.4. Binary Mixtures

Figure 6 shows adsorption isotherms for equimolar mixtures of methane and carbon dioxide at T = 298 K on the four models of activated carbon that we have used for our single-component simulations. As was the case for the single-component isotherms, more carbon dioxide than methane adsorbs on carbons in all cases at the same value of pressure. This behaviour is also predicted from the pure component isotherm, which is obtained by using the DPL mixture model [equation (4)] and IAST [equations (5–8)], respectively—shown as triangles and squares in Figure 6. These curves were calculated using the parameters given in Table 3, obtained by fitting the pure component isotherms to equation (3).

Figure 7 shows the isosteric heats of CO_2 and CH_4 as a function of total loading similar to the conditions described in Figure 6. The isosteric heat of CO_2 and CH_4 is same as that of the pure

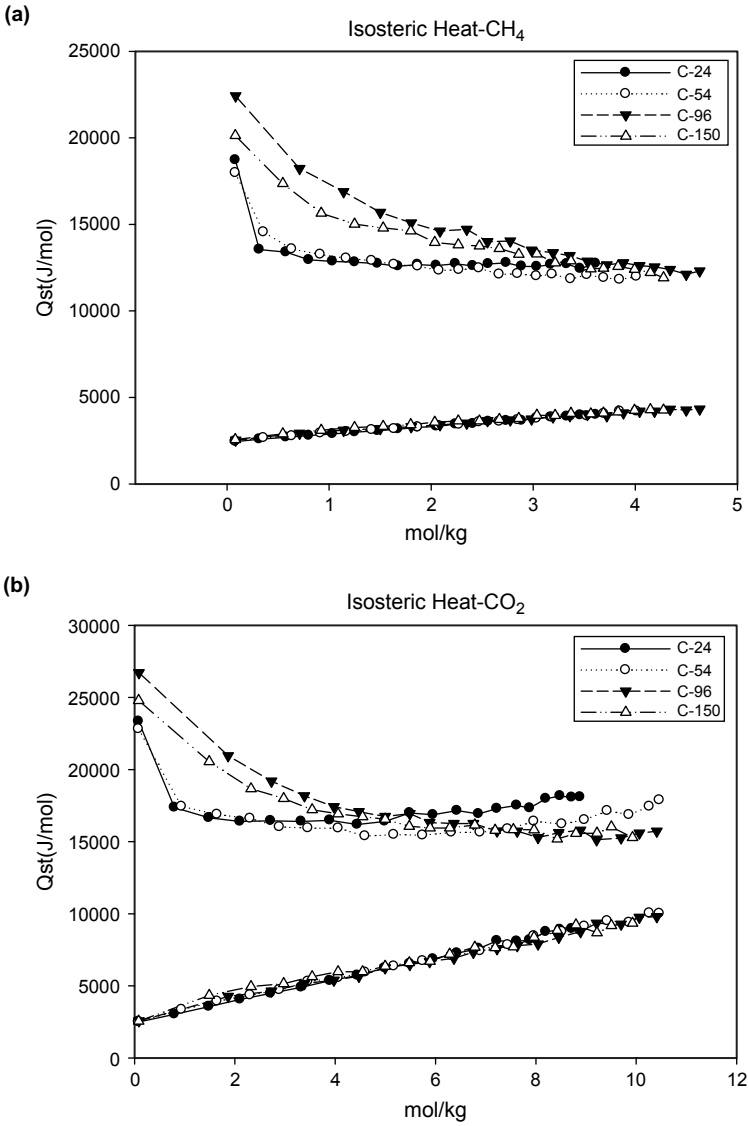

Figure 5. Isosteric heat for the simulated carbons at 298 K (a) CH_4; (b) CO_2.

components (Figure 5). In addition, similar to the pure component results, the qst for both CO_2 and CH_4 initially decreases with increasing total molecular loading, which shows the heterogeneity of the models. This decay continues in the case of carbons C-96-1 and C-150-1. For the C-24-1 and the C-54-1 model, the isosteric heat increases with the loading.

Figure 8 shows the selectivities as a function of total bulk pressure. The simulations results are in good agreement with those obtained experimentally by de Oliveira and co-workers (de Oliveira *et al*. 2011). As observed in the case of isosteric heats, there are two different behaviours in the selectivities of the carbons. First, in the carbons with small clusters (C-24-1 and C-54-1), the

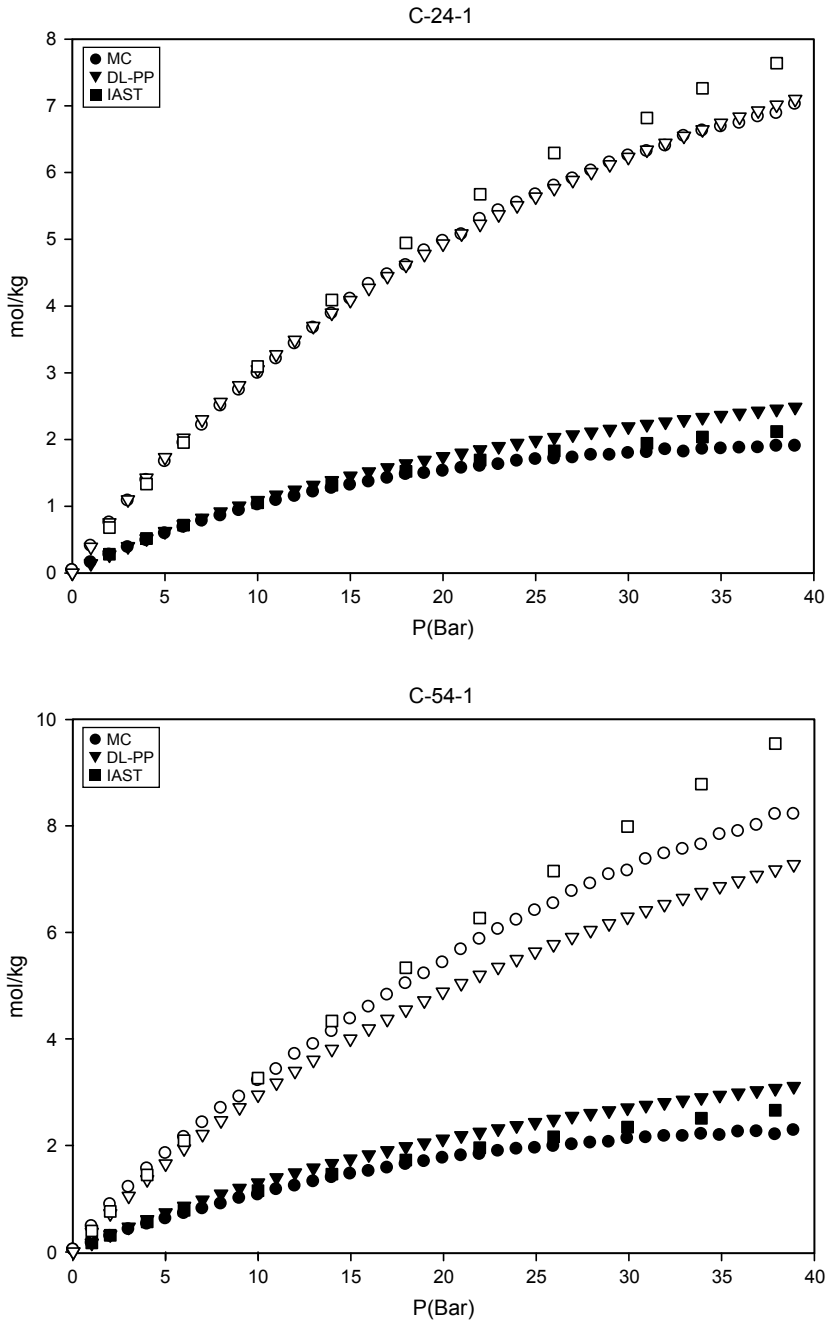

Figure 6. (*Continued*)

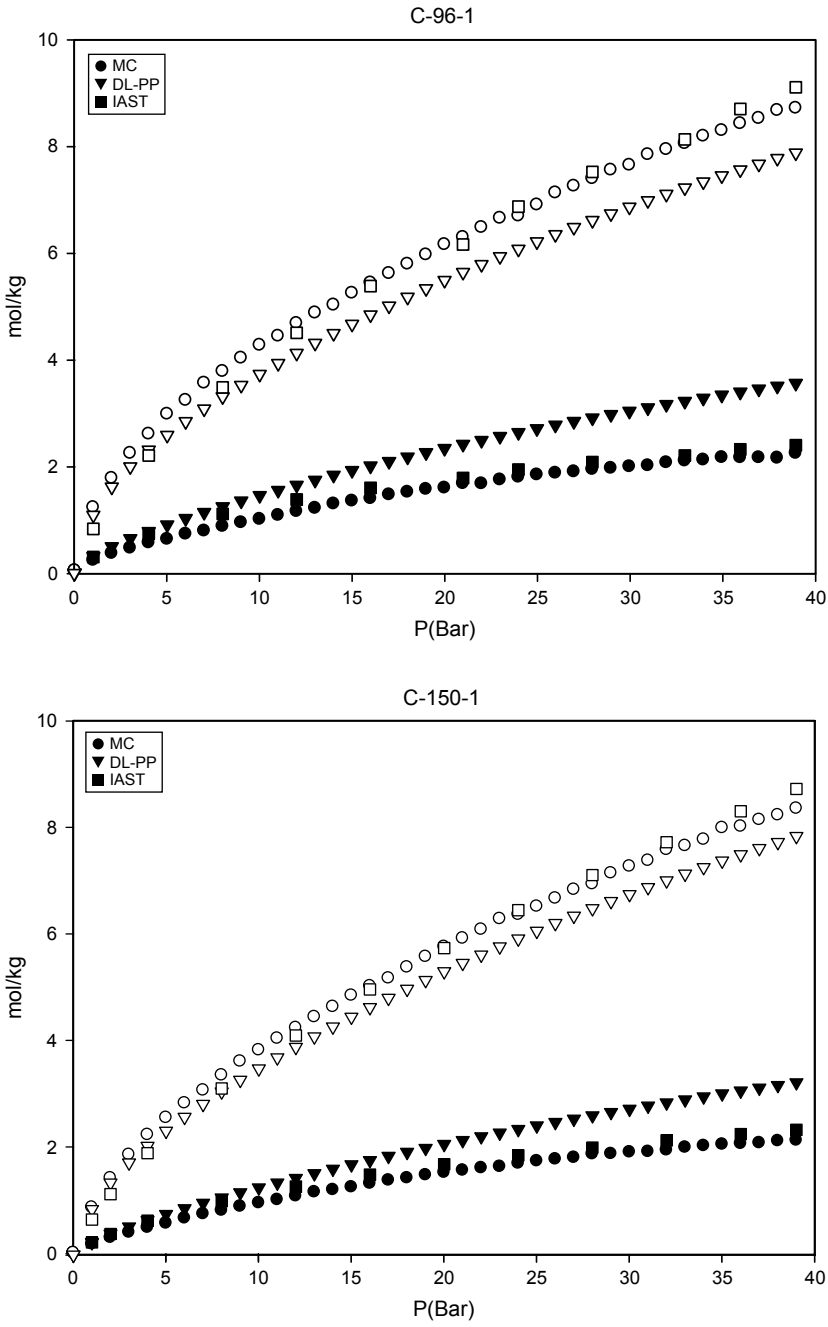

Figure 6. Simulated isotherms (circles) and their fit with dual process Langmuir (triangles) and the ideal adsorption solution theory (squares). The empty symbols correspond to CO_2 and the filled symbols to CH_4. (a) C-24-1; (b) C-54-1; (c) C-96-1; (d) C-150-1.

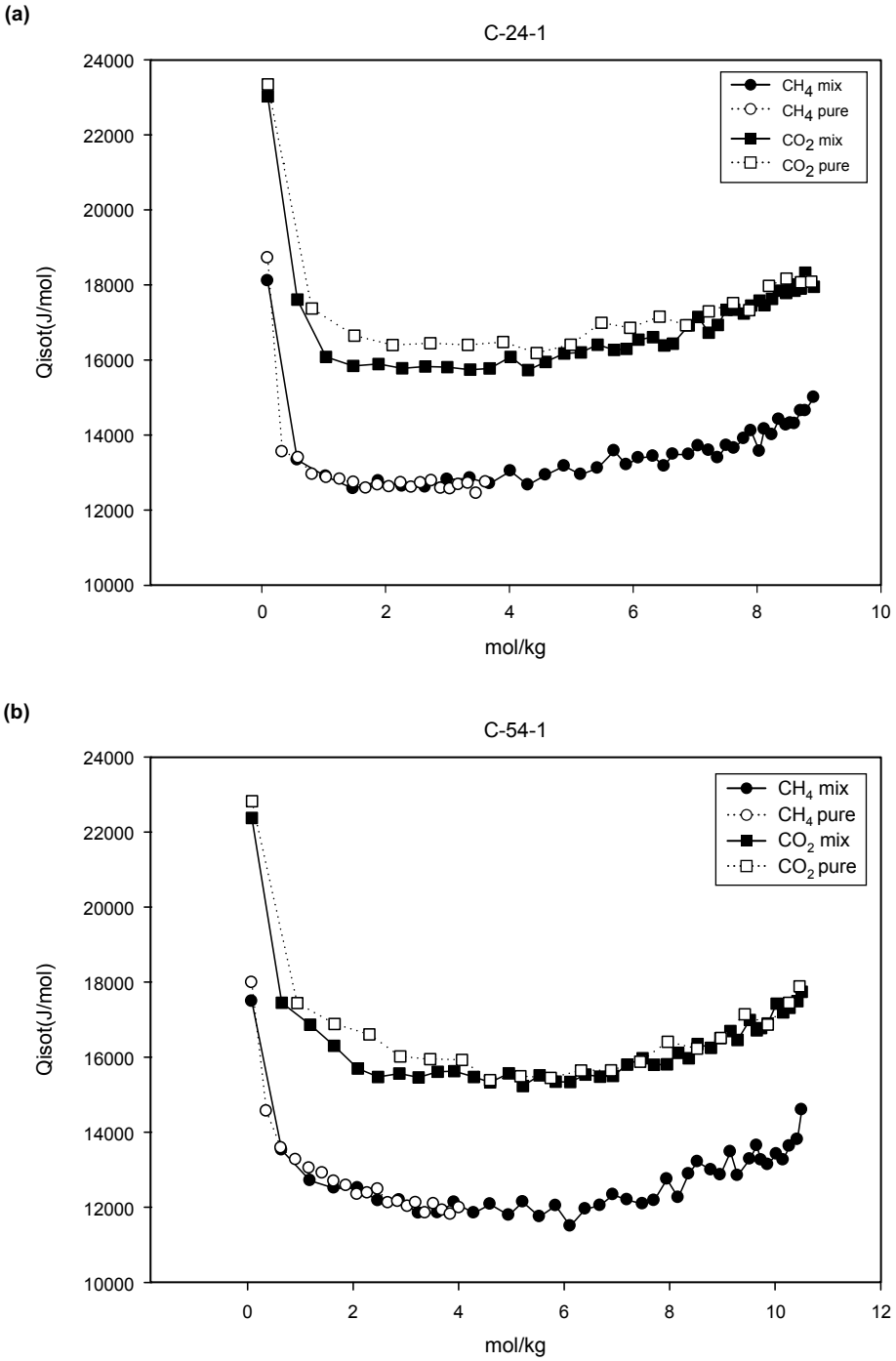

Figure 7. (*Continued*)

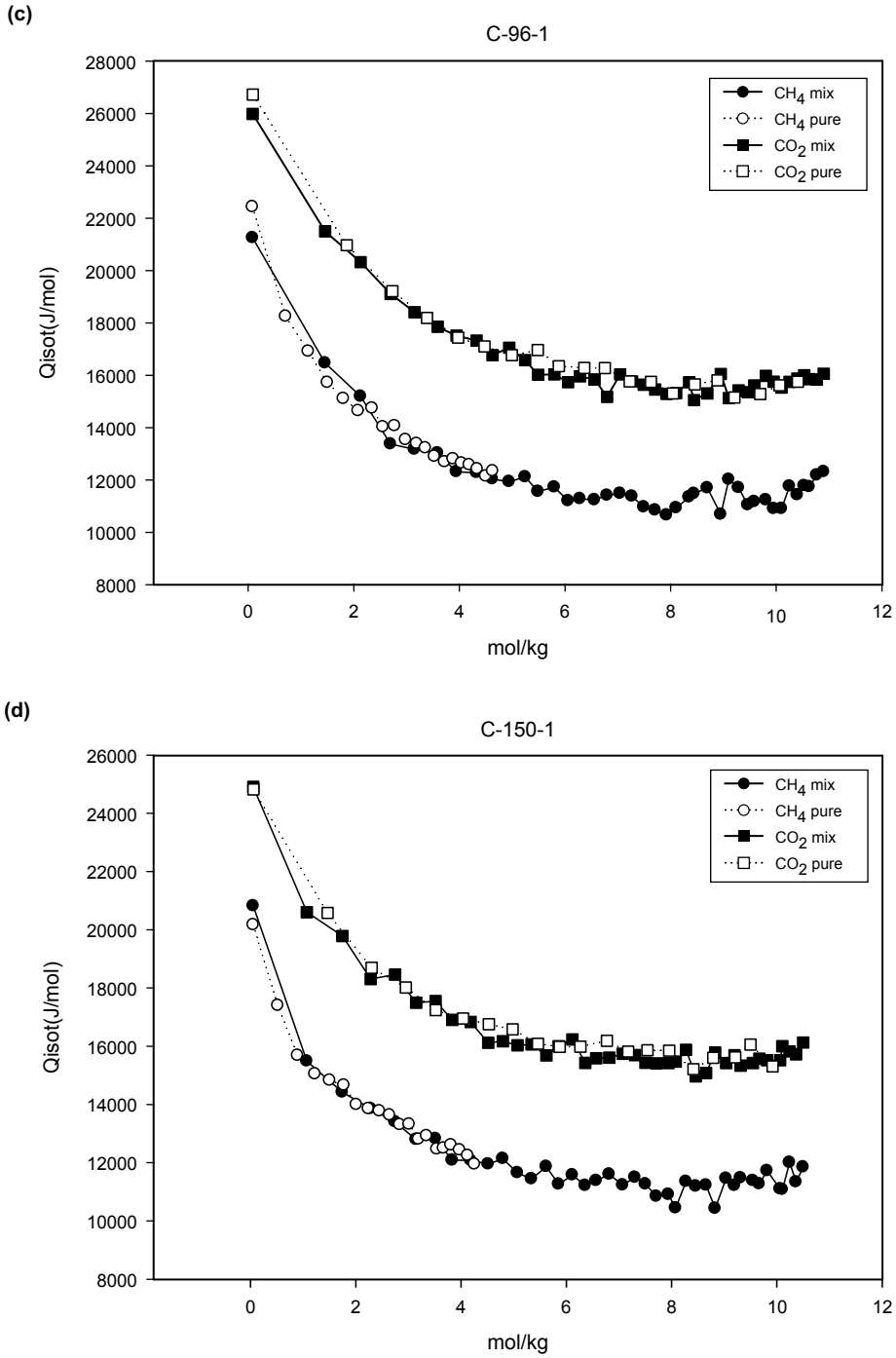

Figure 7. Isosteric heat of adsorption. The empty symbols correspond to the binary mixture and the filled symbols correspond to the unary isotherms. (a) C-24-1; (b) C-54-1; (c) C-96-1; (d) C-150-1.

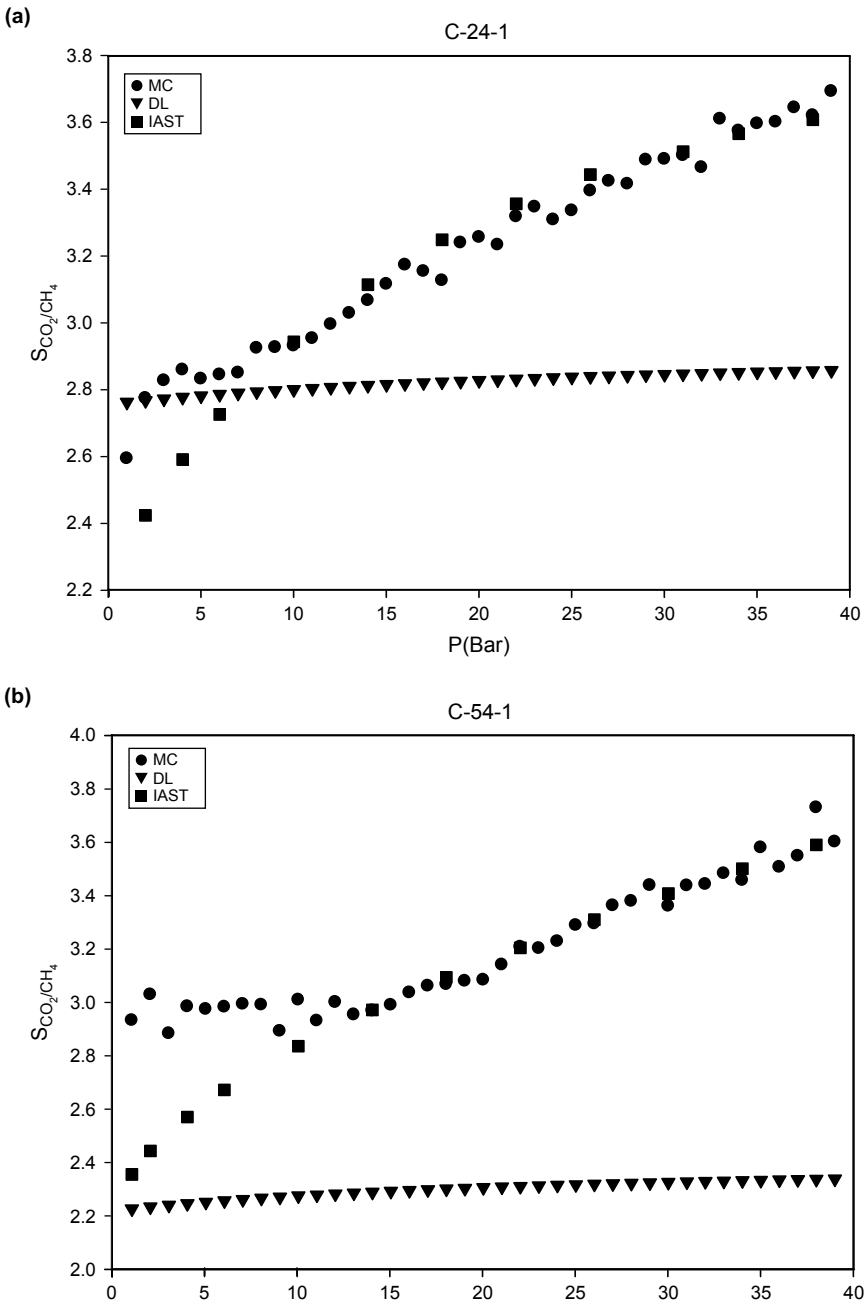

Figure 8. (*Continued*)

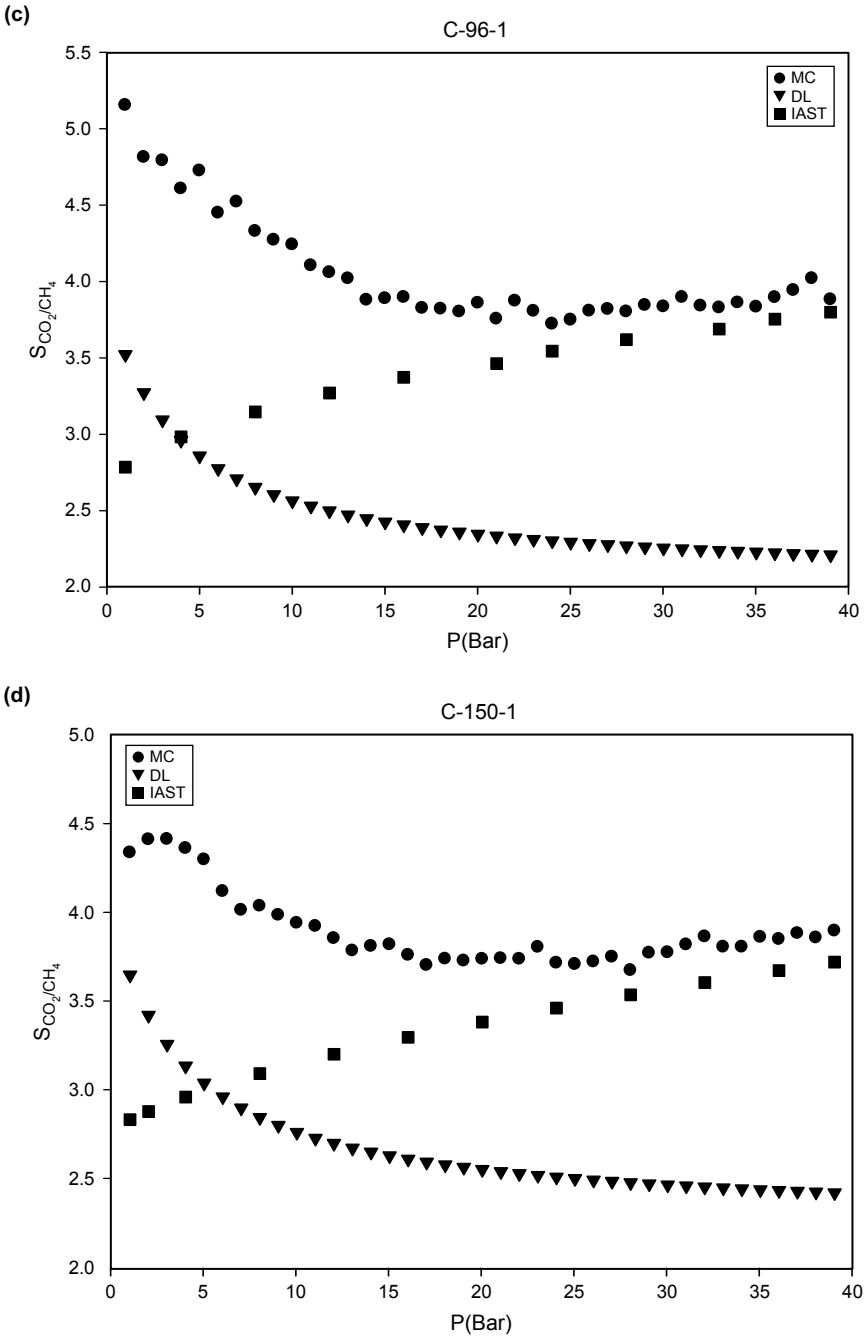

Figure 8. Selectivity of CO_2/CH_4 mixtures using various according to the results of simulation (circles), dual process Langmuir (triangles) and the ideal adsorption solution theory (squares). (a) C-24-1; (b) C-54-1; (c) C-96-1; (d) C-150-1.

selectivity increases with increasing pressure, showing the same behaviour observed in the isosteric heats. The isosteric heat is related to the pore size in the models, with the smaller pores being filled first at low pressures. The carbons C-96-1 and C-150-1 have greater isosteric heats, i.e the greater pores, and thus the selectivity is greater than in carbons C-24-1 and C-54-1. This is because of the fact that in narrow carbon ultramicropores, the equilibrium CO_2/CH_4 selectivity (i.e. preferential adsorption towards CO_2) significantly increased (Kowalczyk *et al*. 2012).

The selectivities in the activated carbon is lower than that obtained on carbon nanotubes (Huang *et al*. 2007), but close to the selectivity in C168 models (Babarao *et al*. 2007). Finally in the coals with large clusters, greater selectivity is observed at low pressures, which tends to decrease with increasing pressure. This demonstrates that the isosteric heat and selectivity are intimately related. It is observed that in all cases the selectivity shows the same numerical value when the pressure becomes large. An important detail is the fact that the dual Langmuir model does not predict the correct numerical value of selectivities; however, it predicts the behaviour qualitatively: an increase in the CO_2/CH_4 selectivity with the pressure in the C-24-1 and C-54-1 models and the decrease in selectivity for the C-96-1 and C-150-1 models. This can be used as a swift method to indicate the adsorption behaviour of mixtures.

4. CONCLUSIONS

In the present work, a molecular model of activated carbon based on clusters of polyaromatic molecules consisting of 24, 54, 96 and 150 carbon atoms and two densities is presented. The model uses an inter-layer separation close to that of graphite. Among the advantages it can be mentioned that, unlike the slit-pore model, it allows to account for pore connectivity and tortuosity in a more realistic way. Parameterization of the isotherms and an analysis of the isosteric heats show that there are two types of sites. At low pressures, preferred adsorption sites are small slit-like pores formed between different clusters, while at higher pressures the pores are constituted by the surfaces and the edges of these clusters. Both DPL and IAST models are suitable to predict the adsorption isotherms of mixtures from pure component data with reasonable accuracy. It has been demonstrated that the isosteric heat and selectivity are intimately related. The dual Langmuir model does not predict correct numerical values for selectivities; however, it predicts the correct behaviour of mixture adsorption, which is very useful for quick assessment of unknown adsorbate–adsorbent systems.

ACKNOWLEDGEMENTS

The authors gratefully acknowledge financial support from the UNLP (Universidad Nacional de La Plata), CICPBA (Comisión de Investigaciones Científicas de la Provincia de Buenos Aires) and CONICET (Consejo de Investigaciones Científicas y Tecnológicas).

REFERENCES

Acharya, M., Strano, M.S., Mathews, J.P., Billinge, S.J.L., Petkov, V., Subramoney, S. and Foley, H.C. (1999) *Philos. Mag. B* **79**,1499.

Albesa, A.G. (2010) *Av. Cienc. Ing.* **1**, 47.

Albesa, A.G., Llanos, J.L. and Vicente, J.L. (2008) *Langmuir* **24**, 3836.
Albesa A.G., Rafti, M., Rawat, D.S., Vicente, J.L. and Migone, A.D. (2012) *Langmuir* **28**, 1824.
Ayappa, K.G. (1998) *Chem. Phys. Lett.* **282**, 59.
Azizian, S. and Bashiri, H. (2009) *Langmuir* **25**, 2309.
Babarao, R., Hu, Z.Q., Jiang, J.W., Chempath, S. and Sandler, S. I. (2007) *Langmuir* **23**, 659.
Bandosz, T.J., Biggs, M.J., Gubbins, K.E., Hattorl, Y., Iiyama, T., Kaneko, K., Pikunic, J. and Thomson, K.T. (2003) Molecular models of porous carbon. In: Radovic, L.R. Ed. *Chemistry and Physics of Carbon,* Vol 28, Marcel Dekker, New York, 41.
Bottani, E.J. (1999) *Langmuir* **15**, 5574.
Buriana, A., Ratusznaa, A., Doreb, J.C. (1998) *Carbon*: **36**, 1613
Coasne, B., Pikunic, J.P., Pellenq, R.J.M. and Gubbins, K.E. (2003) *Mater. Res. Soc. Symp. Proc.* **790**, 53–58.
Dahn, J.R., Xing, W. and Gao, Y. (1997) *Carbon* **35**, 825.
de Oliveira, J.C.A, Rios, R.B., López, R.H., Peixoto, H.R., Cornette, V., Torres, A.E.B., Cavalcante Jr., C.L., Azevedo, D.C.S. and Zgrablich, G. (2011) *Adsorpt. Sci. Technol.* **29**, 651.
Do, D.D. and Do, H.D. (2003), *Adsorpt. Sci. Technol.* **21**, 389.
Do, D.D. and Do, H.D. (2005) *J. Phys. Chem. B* **109**, 19288.
Grabowski, K., Patrykiejew, A. and Sokolowski, S. (2000). *Thin Solid Films* **379**, 297.
Huang, L.L, Zhang, L.Z., Shao, Q., Lu, L.H., Lu, X.H., Jiang, S.Y. and Shen, W.F. (2007) *J. Phys. Chem.* C **111**, 11912.
Karavias, F. and Myers, A.L. (1991) *Langmuir* **7**, 3118.
Kowalczyk, P., Gauden, P.A, Terzyk, A.P., Furmaniak, S. and Harris, P.J.F (2012) *J. Phys. Chem. C*, **116**, 13640.
Kruk, M., Patrykiejew, A. and SokoŁowski, S. (1995) *Surf. Sci.* **340**, 179.
Kumar, A., Lobo, R.F. and Wagner, N.J. (2005) *Carbon* **43**, 3099.
Kumar, K.V., Salih, A., Lu, L., Müller, E.A. and Rodríguez-Reinoso, F. (2011) *Adsorpt. Sci. Technol.* **29**,799.
Kumar, K.V., Müller, E.A. and Rodríguez-Reinoso, F. (2012) *J. Phys. Chem. C* **116**, 11820.
Lee, C.S and O'Connell, J.P. (1974) *Ind. Eng. Chem. Fundam.* **13**, 165.
Myers, A.L. and Prausnitz, J.M. (1965), *AIChE J.* **11**, 121.
Nguyen, T.X., Cohaut, N., Bae, J.-S. and Bhatia, S.K. (2008); *Langmuir* **24**, 7912.
Nieszporek, K (2006) *Langmuir* **22**, 9623.
Palmer, J.C. and Gubbins, K.E. (2012) *Microporous Mesoporous Mater.* **154**, 24.
Palmer, J.C., Brennan, J.K., Hurley, M.M., Balboa, A. and Gubbins, K.E. (2009) *Carbon* **47**, 2904.
Pikunic, J., Lastokie, C.M. and Gubbins, K.E. (2003) *Handbook of Porous Solids* Schuth, F., Sing, K., Weitkamp, J., Eds, Wiley-VCH, Weinheim, Germany, 182.
Ravikovitch, P., Vishnyakov, A. and Neimark, A. (2001), *Phys. Rev. B* **64**, 11602.
Seaton, N.A., Friedman, S.P., MacElroy, J.M.D., Murphy, B.J. (1997) *Langmuir*, **13** 1199.
Segarra, E.I. and Glandt, E.D. (1994) *Chem. Eng. Sci.* **49**, 2953.
Sircar, S (2006) *Ind. Eng. Chem. Res.* **45**, 5435.
Smith, M.A., Foley, H.C. and Lobo, R.F. (2004) *Carbon* **42**, 2041.
Takaba, H., Matsuda, E., Nair, B.N. and Nakao, S. (2002) *J. Chem. Eng. Jpn.* **35**, 1312.
Thomson, K.T. and Gubbins, K.E. (2000) *Langmuir* **16**, 5761.
Woywod, D. and Schoen, M. (2003) *Phys. Rev. E* **67**, 026122.